Primljen / Received: 7.7.2013.
Ispravljen / Corrected: 5.2.2014.
Prihvaćen / Accepted: 4.3.2014.
Dostupno online / Available online: 10.5.2014.

Bond behavior of the reinforcement bar in glass fiber-reinforced polymer connector

Authors:

Kiarash Koushfar, PhD. Candidate
Universiti Teknologi Malaysia
Faculty of Civil Engineering
kiarash.frp@gmail.com

Assoc.Prof. Ahmad Baharuddin Abd. Rahman
Universiti Teknologi Malaysia
Faculty of Civil Engineering
baharfka@gmail.com

Yusof Ahmad, PhD. CE.
Universiti Teknologi Malaysia
Faculty of Civil Engineering
a-yusof@utm.my

Assoc.Prof. Mohd Hanim Osman
Universiti Teknologi Malaysia
Faculty of Civil Engineering
mhanim@utm.my

Scientific paper - Preliminary note

Kiarash Koushfar, Ahmad Baharuddin Abd. Rahman, Yusof Ahmad, Mohd Hanim Osman

Bond behavior of the reinforcement bar in glass fiber-reinforced polymer connector

This paper presents the bond stress – slip behavior of a newly developed grouted splice connection fabricated by glass fiber-reinforced polymer (GFRP). A total of twenty seven specimens were tested under increasing axial tension load. Results from the test specimens were adapted to model a bond stress – slip law to be compared with the requirements provided by design codes and provisions. The results show that by reducing mid-length diameter, higher bond strength and load capacity are generated in the tapered splice sleeves.

Key words:
Splice connector, glass fiber-reinforced polymer, bond stress, slip, precast connection

Prethodno priopćenje

Kiarash Koushfar, Ahmad Baharuddin Abd. Rahman, Yusof Ahmad, Mohd Hanim Osman

Prionljivost armaturne šipke u spoju od polimera armiranog vlaknima

U ovom se radu prikazuje ispitivanje prianjajna i proklizavanja armaturne šipke u novorazvijenoj injektiranoj spojnici sa staklenim vlaknima (eng. glass fiber-reinforced polymer - GFRP). Ukupno dvadeset sedam uzoraka ispitano je postupnim povećavanjem osnog vlačnog opterećenja. Rezultati dobiveni ispitivanjem uzoraka usvojeni su za modeliranje ovisnosti naprezanje prianjanja - proklizavanje, što je uspoređeno sa zahtjevima iz normi i odredbi. Rezultati pokazuju da se u konusnim spojnicama razvija veća čvrstoća prianjanja i otpornost na opterećenje usporedo sa smanjenjem promjera u srednjem dijelu.

Ključne riječi:
spojnica, polimer armiran staklenim vlaknima, naprezanje prianjanja, proklizavanje, predgotovljeni spoj

Vorherige Mitteilung

Kiarash Koushfar, Ahmad Baharuddin Abd. Rahman, Yusof Ahmad, Mohd Hanim Osman

Verbundverhalten von Bewehrungsstahl in Verbindungen aus glassfaserverstärktem Polymer

In dieser Arbeit wird das Haft- und Rutschverhalten einer neu entwickelten mit glassfaserverstärktem Polymer (GFRP) verarbeiten Spleißverbindung dargestellt. Insgesamt sind siebenundzwanzig Proben unter steigenden axialen Zugkräften untersucht worden. Der Einfluss wichtiger Parameter, wie z.B. des inneren Durchmessers der GFRP Verbindung und der Anzahl verwendeter Lagen aus GFRP, ist überprüft worden. Die Versuchsresultate sind angewandt worden, um ein Haftungs- und Rutschverhaltensgesetz aufzustellen und das gegebene Model mit den Anforderungen bestehender Regelwerke und Bestimmungen zu vergleichen.

Schlüsselwörter:
Spleißverbindung, glassfaserverstärktes Polymer, Haftspannung; Rutschverhalten, Fertigteil-Anschluss

1. Introduction

Several methods are available to splice reinforcing bars, including clamping, welding, threaded sleeves and grouted systems. Grouted systems are used extensively in precast concrete structures and are capable of providing reinforcing bar tension and compression splice capacities equal to 150 percent of the specified yield of the bars [1].
The splicing mechanism is typically a cylindrical steel sleeve with open ends where the reinforced bar can be inserted. Once the bar is in place, a specially formulated non-shrink grout with high initial strength is pumped into the sleeve by way of PVC tubes attached to inlet and outlet grouting ports on the sleeves. Special preparation of the bar ends is not required. The bar ends may be separated up to 25 mm. A variation of the system is a sleeve with internal threads at one end, which allows a threaded reinforcing bar to be securely connected to the sleeve. The opposite end of the steel sleeve is open for bar insertion and grouting (Figure 1).

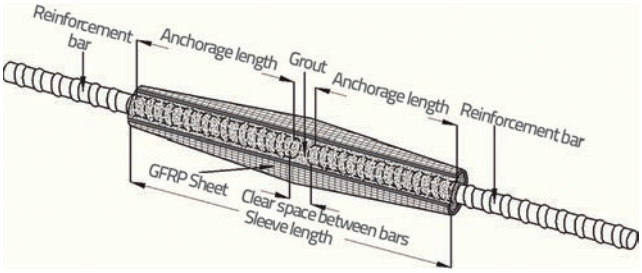

Figure 1. Grouted sleeve connector

The effectiveness of the splice sleeve connector depends on the bond strength between the grout and reinforcing bar. In general, a bond is the interaction mechanism that enables force transfer between reinforcing bars and the surrounding concrete and, therefore, secures composite action between the two materials.
There are three principal elements that contribute to bond resistance: chemical adhesion, frictional resistance, and mechanical interlock due to bearing action between bar ribs and concrete. Adhesion occurs due to the chemical bonding between the cement and the bar as well as the effect of shrinkage stresses that develop during curing; moreover, adhesion depends on the properties of the material around the bar [2].
The frictional resistance and bearing action become effective after the chemical adhesion breaks down. The frictional resistance of the bar-concrete interface against slip is enhanced with the presence of radial pressure on the lateral bar surface [3]. Confinement provided to the anchorage bond zone is an important factor that improves the bond resistance [4, 5, 6]. Confinement can be achieved by applying normal pressure in a direction perpendicular to the applied axial stress in the reinforcing bars [7, 8].

In the construction industry, the primary cause of corrosion in steel joint connectors is exposure to sodium chloride that is present in marine environments or de-icing salts that are applied to bridge decks and parking structures. The current mechanical connections are susceptible to corrosion, which could lead to deterioration of the strength of the structure. Therefore, the construction industry needs to seek alternatives to steel components; a potential solution is the use of FRP materials as conventional steel connectors. FRP materials have the potential to be viable alternatives to conventional steel joint connections because their material properties provide them a significant advantage over steel in terms of weight, durability, and corrosion resistance.
In this experimental study, GFRP sleeves were designed to resist tensile load in the connected steel bars. The sleeve connector is proposed as an alternative to the current metallic sleeves to join precast concrete members. The research investigated the effects of mid-length diameter of the GFRP connector, and the number of GFRP layers to the performance of the connector by investigating the bond stress – slip behavior between the steel bars and grout.

2. Experimental program

The study investigates the bond strength–slip behavior of steel reinforcement bars spliced with tapered GFRP sleeves under incremental axial tension load. The dimensions of the specimens, such as the mid-length diameter of the connector, were monitored. The tests were conducted by fixing the specimen in the tensile test apparatus. A Dartec 500 kN Servo Hydraulic Testing Machine was used for the test program. The rate of loading was set to 0.2 kN/sec for all tests and was controlled by a system controller. A total of 18 GFRP tapered sleeve and 9 steel pipes as control specimens were tested under an increasing axial tension load. The results from the control specimens were compared with those of the GFRP sleeves to study the effect of changes in mid-length diameter of the GFRP sleeve and type of confining material on the bond behavior of the grouted splice connector. All GFRP sheets employed the same epoxy as the matrix.

2.1. Material properties

All specimens were produced from the same GFRP sheets, epoxy resin, grout. Sika grout-215 was used in this experimental program. It is a pumpable dual-shrinkage compensated, self-leveling, cementitious grout with an extended working time to suit local ambient temperatures. The average grout strength of Sika grout-215 is approximately 47.86 N/mm^2 after 7 days of curing.
All steel reinforcement bars used in this experimental study had similar geometrical properties: 16 mm in diameter with an average cross-sectional area of 201.06 mm^2, BS4449 Grade 460 and a bar rib pattern of deformed type 2 [9]. The average tensile strength of the steels, as obtained from 3 single bar

tensile tests, is 573.95 N/mm^2, with an ultimate failure load of 115.40 kN, and the minimum yield strength is 489.90 N/mm^2. The WOVEN ROVING XD-600 GFRP sheets were employed in the study (Figure 2). Woven Roving (WR) consists of glass roving, which is woven into a cloth, with a plain weave directional construction. WR involves bi-directional reinforcements constructed from untwisted fibers in parallel rows with a wrap array (roll direction) interspersed with a weft array (width of roll).

The unsaturated epoxy resin EPICOTE 1006 SYSTEM is an isophthalic resin, which is formulated especially for the tropical climates. The resin ingredient was mixed in a room environment according to manufacturer specifications. The resin was pigmented by adding up to 60% of EPICOTE 1006 Hardener Part B, and tests were conducted to ensure that adding the pigment paste does not impair the performance of the laminate. Resin was used in this study because it had the following properties: it was compatible with glass fibers and had low viscosity to achieve the good fiber wet-out during the process, a fast cure time and low cost..

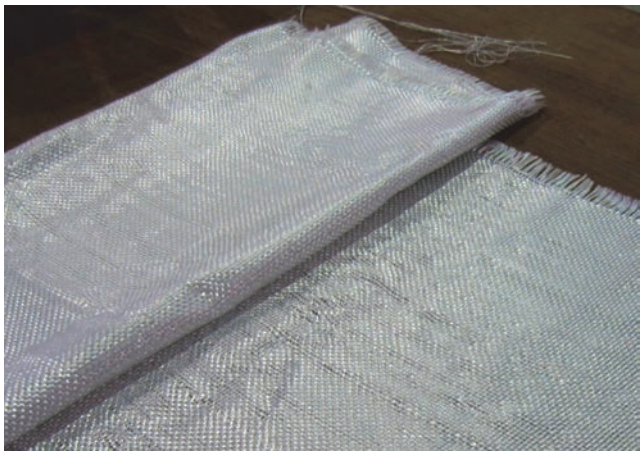

Figure 2. Woven roving GFRP sheet

2.2. Test specimens

The control specimen and tapered GFRP connector are shown in Figure 3 and Figure 4, respectively. The specimens were configured with different sleeve diameters and number of GFRP layers to study the effects on the bond performance. Three identical specimens were prepared for each configuration. All specimens had an overall length (L_s) of 360 mm and diameter of 35 mm at both ends (D_o).

Figure 3. Steel cylindrical control specimen

Nine control specimens without interlocking mechanism on the sleeves were tested to be compared with the test results of the GFRP specimens. The thickness of the mild sleeve pipes used for control specimens was 4 mm.

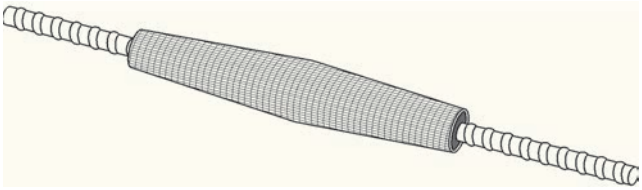

Figure 4. GFRP grouted sleeve connector

The GFRP connector was fabricated by wrapping 4 and 5 layers of GFRP sheets around the tapered shaped plastic moulds to have similar thickness as the steel pipe (see Figure 5). Two, 400 mm long, 16mm diameter deformed high strength steel bars were used for each specimen. One end of each reinforcement bar was spliced together end-to-end in a tapered GFRP sleeve, and the other ends were free. The bars were spliced together with Sika grout-215 in the tapered GFRP coupler. The main variables of this experimental study are:

a) Mid-length diameter of the GFRP sleeve: 50 mm, 65 mm, and 75 mm.
b) Number of FRP layers: 4 and 5 layers were used for each series of specimens.

According to the variables, G5-D50 refers to the specimen which is confined by 5 layers of GFRP sheets and having its mid-length diameter of 50 mm. The details of the variables are shown in Figure 6 and Table 1.

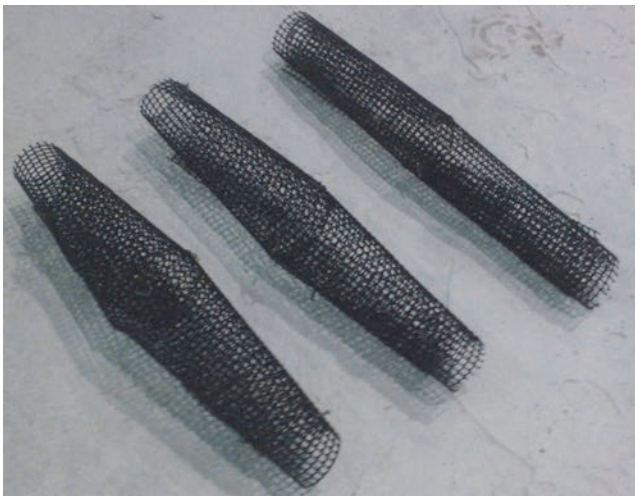

Figure 5. Plastic moulds

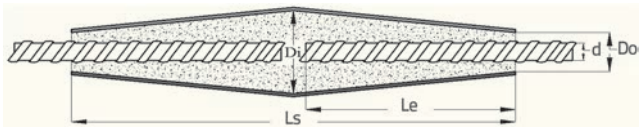

Figure 6. Dimension of the variables

Table 1. Geometrical properties of specimens

Specimen	No. of GFRP layers	Di [mm]	Do [mm]	Clear cover at mid-length, c [mm]	Sleeve material
C-D50	–	50	50	$1{,}06 \cdot d_b$	steel
C-D65	–	65	65	$1{,}53 \cdot d_b$	steel
C-D75	–	75	75	$1{,}84 \cdot d_b$	steel
G5-D50	5	50	30	$1{,}06 \cdot d_b$	GFRP
G4-D50	4	50	30	$1{,}06 \cdot d_b$	GFRP
G5-D65	5	65	30	$1{,}53 \cdot d_b$	GFRP
G4-D65	4	65	30	$1{,}53 \cdot d_b$	GFRP
G5-D75	5	75	30	$1{,}84 \cdot d_b$	GFRP
G4-D75	4	75	30	$1{,}84 \cdot d_b$	GFRP

Sleeve length Ls = 22.5 · d_b = 360 mm, steel bar diameter d_b = 16 mm, steel bar embedded length Le = 4.69 · d_b = 75 mm, and infill material: Sika grout-215.

2.3. Test setup

The specimens were tested using the Dartec Universal Testing Machine (see Figure 7.a). A pair of wedge pressured grips was used to hold specimens vertically. Also, the wedges effectively provided sufficient lateral pressure to prevent slippage between the grip face and steel bars extruding from the GFRP sleeve. The stress-strain and slip readings were taken after the wedges had properly gripped the specimens.

Tapered GFRP sleeve connectors were subjected to an incremental tensile load to record the stress-strain relation of the bar splices as well as the slip that occurs in the bar-to-GFRP connection. Two strain gauges were installed on the spliced steel bars at the distance of one bar diameter, d, from the grouted sleeve end to measure the tensile strain in the steel bar. The placement of the strain gauges was based on the recommendations by ASTM A1034 [10]. Also, one strain gauge was installed at the mid-length of the GFRP sleeve to study the longitudinal behavior of the sleeve under incremental tensile load. The placements of the three strain gauges are illustrated in Figure 7.b.

To measure the slippage of the connected steel bars, one LVDT (low voltage displacement transducer) was placed below the L-shaped steel angle that was attached to the steel bar see Figures 7.a and 7.b. The magnetic base of the LVDT was mounted to the unmovable lower grip. As the tensile load was applied, the upper grip pulled the specimen upward. The slippage values of steel bar under increasing axial load were monitored, by recording the vertical displacement of the L-shaped steel angle using the LVDT.

Prior to the tests, the samples were placed in room environment at 27±2 °C temperature and 70±5 relative humidity for seven days to condition and cure the epoxy resin. After curing, the specimens were ready for performance tests. Compressive tests were conducted on the 100 mm cubes of grout on the 7th day of curing to determine the 7 day compressive strength of the grout.

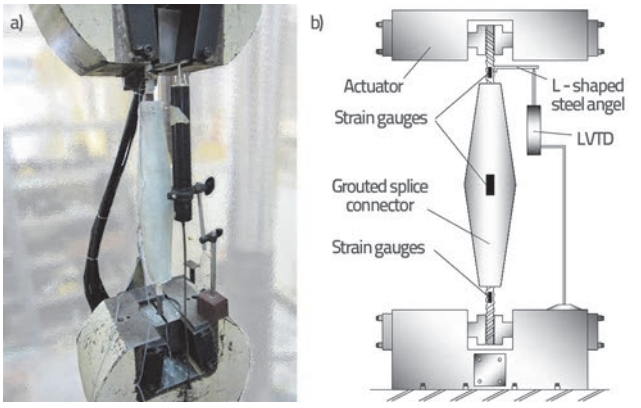

Figure 7. Sample configuration and test setup: a) Tensile test setup; b) LVDT and strain gauges placement

3. Analysis of the test results

3.1. Bond-slip behavior of the specimens

Due to the complexity in detailed estimation of bond strength and presence of a wide range of factors influencing the bond performance [11, 12], the bond stress between the bar surfaces is calculated in accordance with clause 3.12.8.3 BS8110 Part 1 [13] and taken as the force in the bar divided by the surface area that contributes to the anchorage resistance. Assuming a uniform bond stress distribution along the embedment length is an appropriate simplification, given the lack of information on the actual bond stress distribution. Hence, the bond stress can be calculated by using Eq. (1):

$$\tau = \frac{P_U}{\pi \cdot d \cdot L_e} \quad (1)$$

where:

τ - bond stress

P_U - ultimate pull-out load

d - nominal bar diameter
Le - embedment length.

Table 2 presents the test results of ultimate load, ultimate bond stress and the corresponding slip for all specimens. The ultimate bond stresses were calculated based on Eq. (1). The slip values shown in Table 2 and Figures 8 to 11 were obtained directly from the LVDT readings. Except for control specimens, the slip values were contributed by the bar slippage and bar yielding as evident from the steel strain values that had exceeded the yield strain of 0.002 (2000 μm/m), see Figures 9 and 11. At ultimate load level, the steel bars had yielded and then followed by sudden bar pulled-out due to inadequate anchorage length. This resulted in loss of reading and hence the descending curves of the stress-slip were not recorded. This response is similar to research works reported by Abbrishami and Mitchell [14,15]. The slip due to elongation of GFRP sleeve is considered negligible because of the small strain in the GFRP sleeve of less than 0.0006 (600 μm/m), see Figure 13.

Referring to Table 2, the highest bond stress occurred in 50 mm diameter specimens confined with 5 GFRP layers and the lowest bond stress occurred in 75 mm diameter specimens confined with 4 GFRP layers. The maximum bond stress of the control specimens C-D50 was only 9.12 N/mm^2, lower than the bond stress in specimens with GFRP tapered sleeves. This could be due to inadequate radial confinement of the grout in the connectors. The maximum bond stress in specimens

Table 2. Summary of the test results

Specimen	No.	Ultimate load [kN]	Average ultimate load [kN]	Ultimate bond stress, Eq. (1) [N/mm^2]	Average ultimate bond stress [N/mm^2]	Slip [mm]
C-D50	A	33,93		9		1,1
	B	34,21	34,41	9,07	9,12	0,98
	C	35,08		9,3		1,07
C-D65	A	32,44		8,6		1,02
	B	33,06	32,54	8,77	8,63	0,91
	C	32,12		8,52		0,84
C-D75	A	32,11		8,52		0,93
	B	32,72	31,97	8,68	8,48	0,79
	C	31,09		8,25		0,81
G5-D50	A	101,44		26,91		3,4
	B	99,94	99,37	26,51	26,36	3,15
	C	96,74		25,66		3,21
G4-D50	A	89,73		23,8		2,97
	B	87,27	86,31	23,15	22,90	3,06
	C	81,94		21,74		3,09
G5-D65	A	91,53		24,28		2,93
	B	92,23	91,57	24,46	24,29	3,24
	C	90,94		24,12		2,94
G4-D65	A	87,37		23,18		2,74
	B	88,19	86,64	23,39	22,98	3,12
	C	84,36		22,38		3,37
G5-D75	A	87,37		23,4		3,04
	B	89,90	88,49	23,85	23,48	3,26
	C	88,21		23,18		2,81
G4-D75	A	83,96		22,55		2,93
	B	85,01	84,44	22,27	22,40	2,89
	C	84,34		22,37		3,47

G-D50 GFRP tapered sleeve was 26.36 N/mm², approximately three times that of control specimens. This outcome leads to the conclusion that the specimen with a higher load capacity largely is affected by the confinement provided by the tapered GFRP sleeve.

The test results in Table 2 also indicate that as the mid-length diameter of the tapered sleeve increases, the ultimate load and bond strength which the specimen can sustain decreases [16]. It is believed that while the tapered grout successfully transfers the tensile stresses to the tapered sleeve, the smooth internal surface of the tapered GFRP sleeve causes the resistance to be provided solely through the chemical or adhesion bond of the grout, which is not sufficient to sustain the stresses. The smaller mid-length diameters were able to control the propagation of the splitting cracks to increase the bond capacity of the specimen.

The relationship between bond stress – slip as obtained from experimental results are given in Figures 8 to 11. At ultimate states, all the bond stress – slip curves did not show any gradual plateau. The 75mm bar embedded length was not designed to cause fracture in the steel bars, hence a gradual plateau curve did not occur. In this study, it was expected that the chosen 75 mm embedded length was a suitable length to investigate bond stress that would cause bar pullout failure at early load level without bar yielding. However due to significant enhancement of bond mechanism in the tapered sleeve, the bar pullout occurred at higher load levels, to the extent that the steel bars yielded before pulled out, see Figures 14 and 15.

The response of slip is shown in Figures 9 to 11. The high values of slip, mostly greater than 3 mm, were associated with bar pulled out at higher load level. In real application involving this connection, this large slip due to bar pullout can be avoided. To prevent bar pullout, the bar embedded length must be designed by using Eq. (1).

The authors had also conducted testing of the splice specimens with the objective to ensure fracture of the spliced bars. The results show that embedded length of 125 mm with mid-length diameter of 50 mm is required to ensure the GFRP connector could achieve the tensile strength of the steel bar, see Figure 16.c.

3.2. Stress-strain behavior of the specimens

As mentioned previously, all specimens were mounted with strain gauges to measure the longitudinal strains in the bars. Figures 14 and 15 show the average stress-strain curves of three identical specimens of each series in the reinforcement

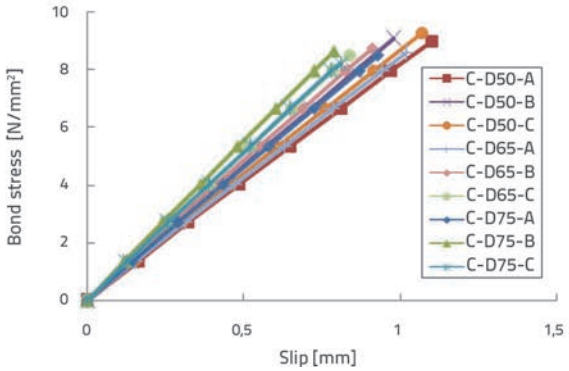

Figure 8. Bond stress – slip between grout and steel cylindrical sleeve for control specimens

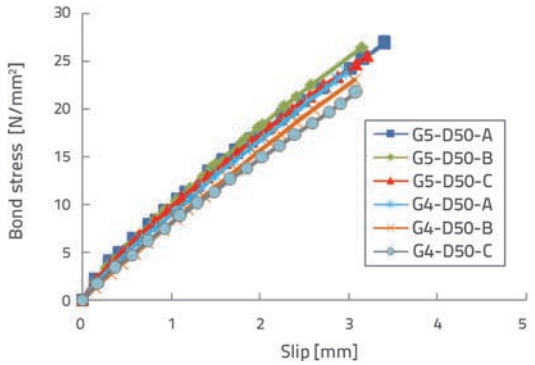

Figure 9. Bond stress – slip of reinforcement bar for 50 mm diameter G5 and G4 series

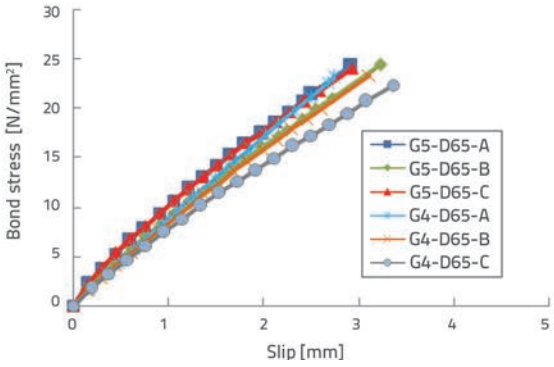

Figure 10. Bond stress – slip of reinforcement bar for 65 mm diameter G5 and G4 series

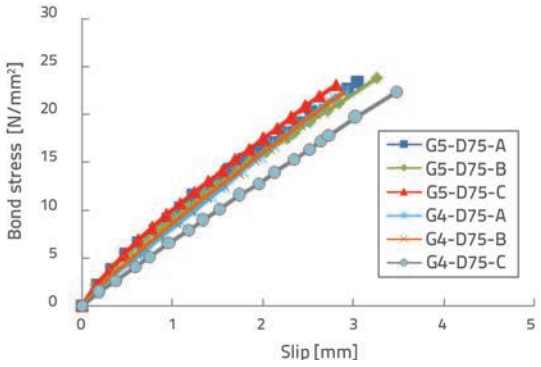

Figure 11. Bond stress – slip of reinforcement bar for 75 mm diameter G5 and G4 series

bars. Referring to Table 2, the ultimate tensile capacities of the GFRP specimens were generally less than 102 kN.

Figure 16(a) shows the failure mode of the control specimen due to the slippage of the grout from the cylindrical steel sleeve, indicating that the bond strength of the sleeve-grout interface is weaker than the bar-grout interface. Furthermore, the strain on the steel sleeve is significantly small, i.e less than 0.0002 (200 μm/m), indicating that very minimum force is transferred to the cylinder steel splice, see Figure 12, due to weak anchorage bond between grout and sleeve. The purpose of the control specimen is to prove that the cylindrical steel splice does not provide any significant contribution in enhancing bond mechanism between sleeve-to-grout and also between bar-to-grout.

On the other hand, as shown in Figure 16(b), the GFRP tapered sleeve had improved the bond between the GFRP sleeve and grout. The steel bars in GFRP tapered specimens had yielded beyond yield strain 0.002 (2000 μm/m), prior to the pullout of the steel bar from the sleeve. There was no pull-out failure of grout from the sleeve. The specimen failed in the bonding between bar and grout, as a result the reinforcement bar slipped out of the GFRP sleeve. This mode of failure occurs as a result of both the wedging action of the steel ribs pushing the surrounding material away and the crushing of the grout keys by the ribs as evident from the bar pullout failure mode. With the sleeve as a means of confinement, the splitting can be retained; thus, the bond failure occurs by shear failure of the grout keys between the steel and ribs. This failure mode indicates that the connection capacity is less than the tensile strength of the reinforcement bar. However, the bar embedment length had generated required bond to allow specimens to fail by yielding before the reinforcement fractured.

Upon slippage of the bar relative to its surroundings, the concrete cover is forced to dilate radially by an amount that can be calculated from the slip magnitude and the geometric profile of the interlocking ribs. Dilation leads to cover splitting, and if there is no mechanism to arrest crack propagation, splitting failure may occur along the anchorage [17]. Dilation generates reactive radial pressures on the bar, which are

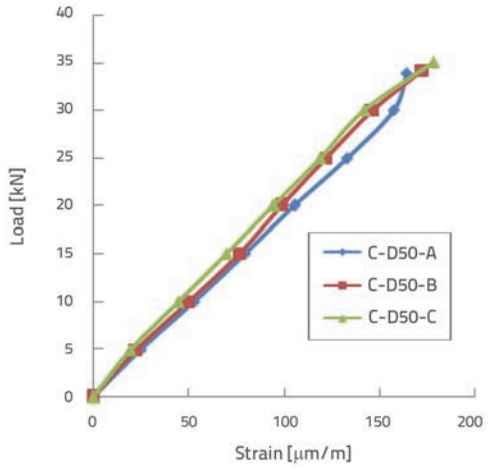

Figure 12.Load-strain in cylindrical steel, control specimens

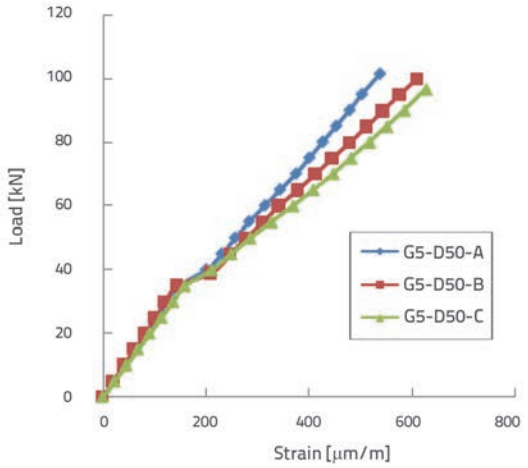

Figure 13. Load-strain in GFRP sheet, tapered GFRP sleeve

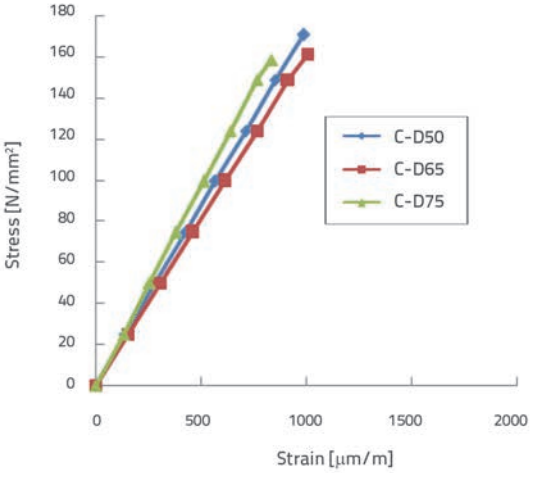

Figure 14. Stress-strain in the bar, control specimens

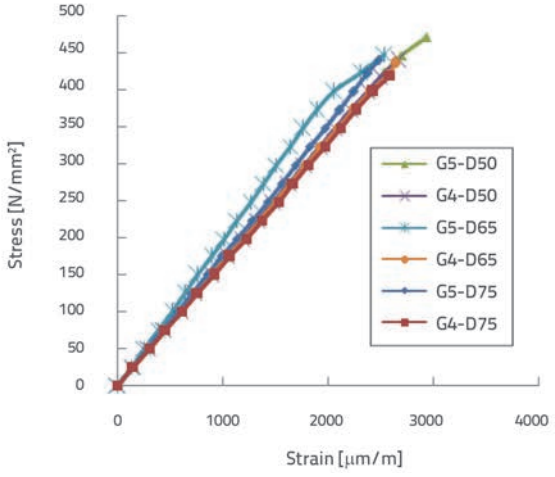

Figure 15. Stress-strain in the bar, GFRP specimens

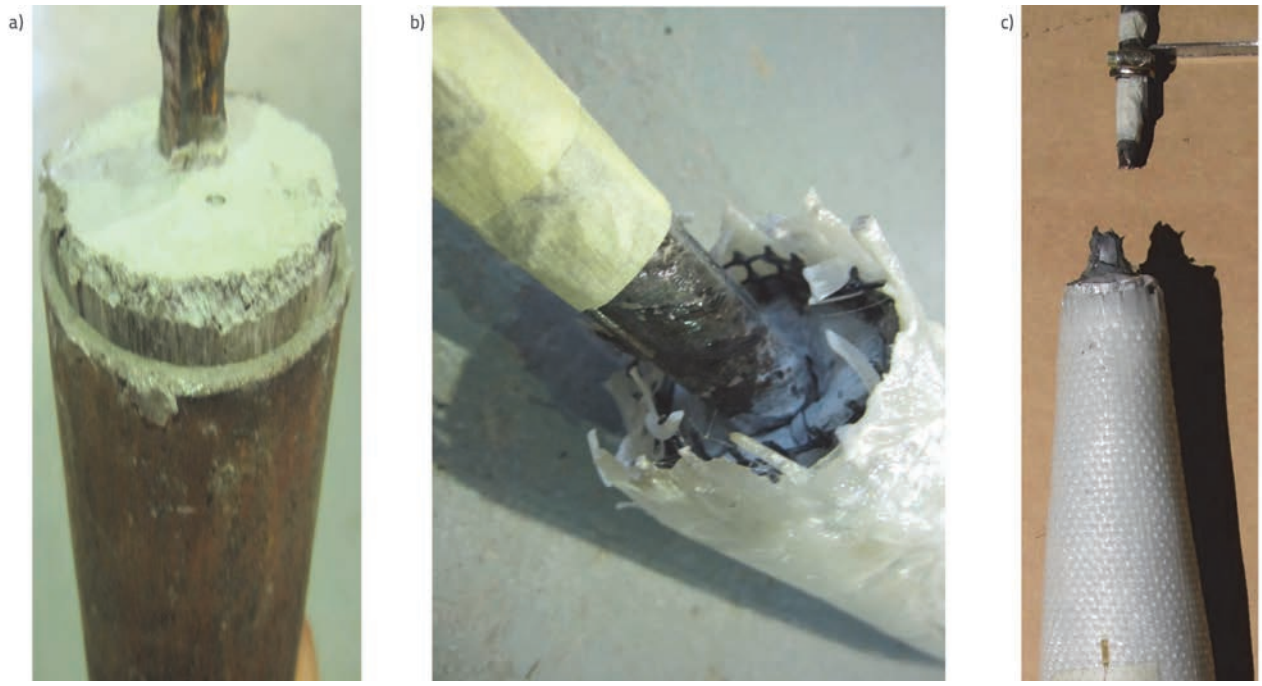

Figure 16. Failure modes of specimens: a) Grout-sleeve interface failure; b) Bar pull-out failure; c) Bar tensile failure

resisted by all available confining mechanisms such as the hoop tension in the concrete cover, the tensile force in the stirrups or the externally bonded composite jackets along the anchorage zone, which are mobilized as they are crossing the splitting plane [18]. If sufficient confinement is available, splitting through the cover may be delayed or even prevented, which leads to a mixed mode of failure that combines partial splitting and bar pullout.

Referring to Figure 17, as a pulling force, P (represented by the arrow) was applied to the reinforcement bar, the reaction stresses at the bar end are uniformly distributed away from the steel bar to the tapered grout. Subsequently, the inclination surface of the tapered grout distributes the stresses in a diagonal direction and transfers these stresses to the tapered GFRP sleeve, which confines the grout [19]. According to the test results, the stresses transferred to the tapered GFRP sleeve are higher than those in conventional steel pipes. Moreover, due to this transfer mechanism, the stresses along the interface of the reinforcement bar with the grout are reduced significantly.

Figure 17. Distribution of the Stresses

3.3. Effects of Tapered Confinement

According to Tighiouartet. al [20], bond strength is determined by the damage of the steel–concrete interface. At the local level, if the stresses exceed the tensile strength of the concrete then the bond strength decreases by crushing of concrete in front of the bar ribs and development of the localized cracks or shearing-off the concrete keys between steel lugs. So, it is reasonable to define bond strength as a function of concrete shear strength or concrete tensile strength. Since both of these quantities typically are approximated as being proportional to the square root of the concrete compressive strength, thus bond strength can be considered as a function of concrete compressive strength.

According to the Eq. (1), it is assumed that the bond characteristics of a reinforcing bar are analytically described by a local relationship, in which a uniform shear stress, τ, is acting on the contact surface between reinforcement bar and concrete, and the slip, s, is the relative displacement between reinforcement bar and concrete. As mentioned before, due to the complexity in detailed estimation of bond strength, the bond stress between the bar surfaces is calculated in accordance to the clause 3.12.8.3 BS8110-Part1 [13]. The code recommends that bond strength between steel and concrete is calculated based on the compressive strength of the concrete as the tensile strength is a function of compressive strength. To find the values of design ultimate anchorage bond stress, British Standard recommends the following formula:

$$f_{bu} = \beta\sqrt{f_{cu}} \quad (2)$$

where, f_{bu} is the design ultimate anchorage bond stress, f_{cu} is the infill compressive strength, and β is a coefficient dependent on the bar type which could be obtained from Table 3.26 BS 8110 Part 1. In this study, the average compressive strength of Sika grout-215, $f_{cu,}$ is approximately 47.86 N/mm^2

and according to Table 3.26 BS 8110, for the type 2 deformed bars in tension, β=0.5. The ultimate anchorage bond stress for unconfined grout as obtained from Eq. (2) is 3.45 N/mm^2, while test results indicate that specimens with 75 mm bar embedment length offered bond strength between 22 and 27 N/mm^2 which are higher than the design ultimate anchorage bond stress, that is about seven times of f_{bu}. It is largely attributed to the higher confinement provided by the tapered GFRP sleeve.

3.4. Modeling of the bond-slip relationship

Due to the lack of specific formulations for different types of reinforcement bars, an analytical description of bond between reinforcement bar and surrounding concrete is required. This analytical method can be described by means of a constitutive bond stress – slip relationship to introduce solution of problems, such as the calculation of the development length.

Eligehausen et al. [21] proposed a well-known bond stress – slip analytical law for deformed steel bars. According to the BPE model, the bond stress – slip of refinement bar shows four distinct branches (Figure 18). The first branch refers to the section in which the ribs placed into the grout matrix, referring to local crushing and micro-cracking. The ascending branch of the BPE model (s ≤ s1) is expressed as follows:

$$\frac{\tau}{\tau_1} = \left(\frac{s}{s_1}\right)^{\alpha} \tag{3}$$

where, τ_1 = maximum bond stress; τ_1= slip corresponding to maximum bond stress, and α is a curve fitting parameter that must not be larger than 1 (α=0.4 for steel bars).

According to Tighiouart et al. [20], who investigated bond in concrete with fiber reinforced polymer bars suggested that the BPE model which is proposed for steel rebars, could be used to express the ascending branch of the bond-slip (s1<bs2) for a specimen in tension.

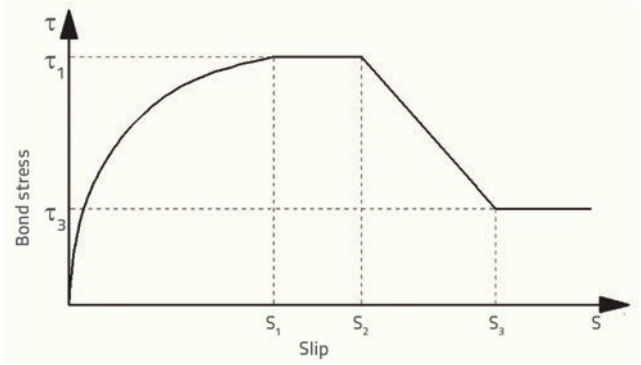

Figure 18. BPE model

In this study term α was calibrated from the experimental data by using the least-square error method and presented by the following equation:

$$\alpha = \left(\frac{d_i}{N_{GFRP}}\right)^{\gamma} \tag{4}$$

The values of α and γ for the specimens are presented in Table 3. The experimental results of bond-slip curves and the calibrated modeled curves for G4-D65 and G5-D75 series are presented in Figure 19. Bond-slip curves indicate that the BPE model provides a slightly conservative approximation by underestimating the bond strength of the specimens.

Table 3. Values used in the BPE model

Specimen	α	γ
G5-D50	0,83	-0,08
G4-D50	0,92	-0,03
G5-D65	0,83	-0,07
G4-D65	0,92	-0,03
G5-D75	0,83	-0,07
G4-D75	0,92	-0,03

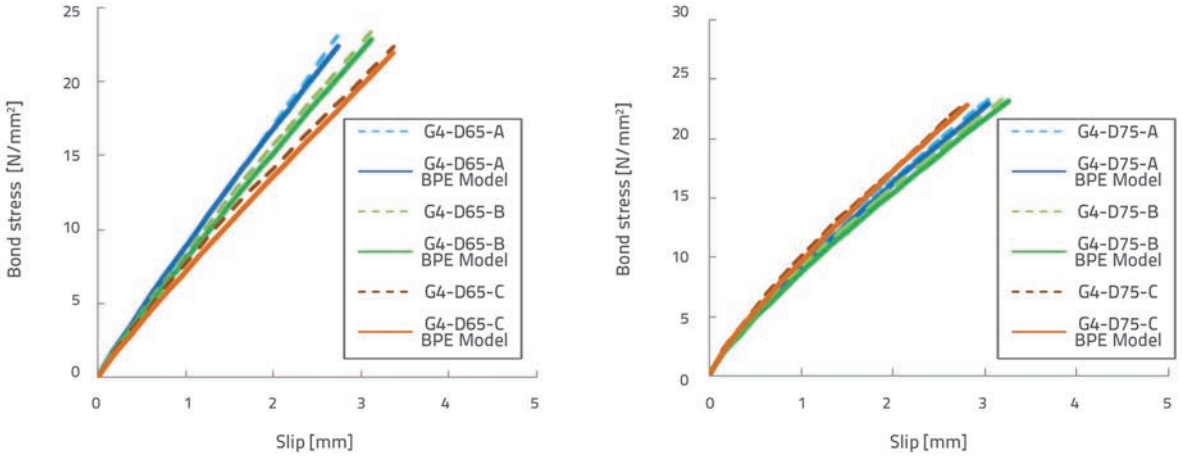

Figure 19. "Stress - slip" curve: a) G4-D65 series; b) G5-D75 series; showing raw and modeled data

4. Conclusion

The objective of the present study was to investigate the effects of the number of GFRP layers and the mid-length diameter of the specimens on the bond behavior of GFRP splice connector. The results were compared with the requirements provided by design codes and provisions. Based on the analysis of the experimental results, new values for the curve fitting parameter were found using a bond stress – slip law. Test results show that the bond stress of the steel rebar could be increased significantly through splice confinement by using a tapered shape sleeve to provide a mechanism to increase the transfer-of-force mechanism between the steel bars, grout, and GFRP sleeve connector. In addition, the following specific conclusions can be made:

- The results show that by decreasing the mid-length diameter of the specimens, higher load capacity and bond strength can be maintained. This fact is observed through comparison of the ultimate tensile capacity and bond strengths between GFRP sleeves and control specimens with the same mid-length diameters and embedment lengths.
- The analysis of test results indicate that British Standard design recommendations provide a large margin for safety for the sufficient development lengths and it be reduced by employing the GFRP sleeve connector.
- Based on the results of the tension tensile tests, 5 GFRP layers are sufficient in generating the required confinement, while the use of 4 layers of GFRP laminates as splice couplers for steel bars is not recommended. This research shows that by using 4 layers of GFRP sheets, additional confinement must be added to provide sufficient load capacity and bond strength.
- Results from the test specimens were used to model the experimental data by the derivation of BPE model. The results indicate that the BPE model slightly underestimates the bond strength of the specimens.

REFERENCES

[1] Martin, L.D., Perry, C.J.: PCI Design Handbook: Precast and Prestressed Concrete, Sixth Edition, 2004.

[2] Cox, J.V., Herrmann, L.R.: Development of a Plasticity Bond Model for Steel Reinforcement, Mechanics of Cohesive-Frictional Materials, (1998) John Wiley & Sons, Ltd., pp.155–180.

[3] Tassios, T.P., Vassilopoulou, I.: Shear transfer capacity along a R.C. crack, under cyclic sliding, Befestigungstechnik Bewehrungstechnik, (Rolf Eligehausenzum 60. Geburtstag), (eds. W. Fuchs, H. W. Reinhardt), Ibidem – Verlag, Stuttgart, (2002) pp. 405–414.

[4] Robins, P.J., Standish, I.G.: The influence of lateral pressure upon anchorage bond, Magazine of Concrete Research,(1984) Volume 36, Issue 129, p.p. 195–202. http://dx.doi.org/10.1680/macr.1984.36.129.195

[5] Einea, A., Yamane, T., Tadros, M.K.: Grout-filled Pipe Splices for Precast Concrete Construction, PCI Journal, (1995) January-February, pp.82–93.

[6] Moosavi, M., Jafari, A., Khosravi, A.: Bond of cement grouted reinforcing bars under constant radial pressure. Cement Concrete Composites, (2005) 27 (11):103–109. http://dx.doi.org/10.1016/j.cemconcomp.2003.12.002

[7] Soroushian, P., Choi, K.B., Park, G.H., et al.: Bond of deformed bars to concrete: effects of confinement and strength of concrete. ACI Material Journal, (1991) , pp. 227–232.

[8] Tibbetts A.J., Oliva, M.G., Bank, L.C.: Durable fiber reinforced polymer bar splice connections for precast concrete structures, Composites & Ploycon, (2009) Tampa, FL USA: American composites manufacturers association.

[9] British Standard Institution, Specification for Carbon steel bars for the reinforcement of concrete, BS 4449 : 1988.

[10] ASTM International, Standard Test Methods for Testing Mechanical Splices for Steel Reinforcing Bars. ASTM A1034/A, 2005.

[11] Cairns, J., Plizzari, G.A.: Towards a harmonised European bond test, Materials and Structures, Vol. 36, (2003), pp. 498–506. http://dx.doi.org/10.1007/BF02480826

[12] CEB-FIP, 'Model Code 1990', Thomas Telford, London, (1993), 437pp., ISBN 0 7277 1696.

[13] British Standard Institution, Structural Use of Concrete BS8110: Part 1: (1997): London, Clauses 3.12.8.3 and 3.12.8.4.

[14] Abrishami, H.H., Mitchell, D.: Analysis of Bond Stress Distribution in Pull-out Specimens, Journal of Structural Engineering, Vol. 122 (1996) 3, pp. 255-261.

[15] Tassios, T.P., Koroneos, E.G.: Local Bond-Slip Relationships by Means if the Moire Method, ACI Journal, Vol. 81 (1984) 1, pp. 27-34.

[16] Ling, J.H., Rahman, A.B.A., Ibrahim I. S., Hamid, Z.A.: Behaviour of grouted pipe splice under incremental tensile load, Construction and Building Materials, 33 (2012), pp. 90–98. http://dx.doi.org/10.1016/j.conbuildmat.2012.02.001

[17] FIB Bulletin 10, International Federation for Structural Concrete (2000).

[18] Tastani, S.P., Pantazopoulou, S.J.: Direct Tension Pullout Bond Test: Experimental Results Journal of structural engineering, Journal of Structural Engineering, ASCE, Vol. 136 (2010) 6. http://dx.doi.org/10.1061/(ASCE)ST.1943-541X.0000159

[19] Dahl, K.L., High Strength Grouted Pipe Coupler. U.S Patent No. 6,192,647, (2001).

[20] Tighiouart, B., Benmokrane, B., Gao, D.: Investigation of Bond in Concrete Member with Fiber Reinforced Polymer (FRP) Bars, Construction and Building Materials, 12 (1998), pp. 453–462. http://dx.doi.org/10.1016/S0950-0618(98)00027-0

[21] Eligehausen, R., Popov, E.P., Bertero V.V.: Local bond stress – slip relationships of deformed bars under generalized excitations. Report No. 83r23, EERC, University of California, Berkeley, 1983.